Too dry to survive: Leaf hydraulic failure in two *Salvia* species can be predicted on the basis of water content

Elisa Abate [a], Andrea Nardini [b], Francesco Petruzzellis [c], Patrizia Trifilò [a,*]

[a] *Dipartimento di Scienze Chimiche, Biologiche, Farmaceutiche ed Ambientali, Università di Messina, Viale Ferdinando Stagno d'Alcontres 31, 98166, Messina, Italy*
[b] *Dipartimento di Scienze della Vita, Università di Trieste, Via L. Giorgieri 10, 34127, Trieste, Italy*
[c] *Dipartimento di Scienze AgroAlimentari, Ambientali e Animali, Università di Udine, Via delle Scienze 91, 33100, Udine, Italy*

ARTICLE INFO

Keywords:
Climate change
Leaf hydraulic failure
Leaf shrinkage
Mediterranean species
Membrane damages
Rehydration capacity
Water content

ABSTRACT

Global warming is exposing plants to increased risks of drought-driven mortality. Recent advances suggest that hydraulic failure is a key process leading to plant death, and the identification of simple and reliable proxies of species-specific risk of irreversible hydraulic damage is urgently required.

We assessed the predictive power of leaf water content and shrinkage for monitoring leaf hydraulic failure in two Mediterranean native species, *Salvia ceratophylloides* (*Sc*) and *S. officinalis* (*So*).

The study species showed significant differences in relative water content (RWC) thresholds inducing loss of rehydration capacity, as well as leaf hydraulic conductance (K_L) impairment. *Sc* turned out to be more resistant to drought than *So*. However, *Sc* and *So* showed different leaf saturated water content values, so that different RWC values actually corresponded to similar absolute leaf water content. Our findings suggest that absolute leaf water content and leaf water potential, but not RWC, are reliable parameters for predicting the risk of leaf hydraulic impairment of two *Salvia* species, and their potential risk of irreversible damage under severe drought. Moreover, the lack of any K_L decline until the turgor loss point in *Sc*, coupled to consistent leaf shrinkage, rejects the hypothesis to use leaf shrinkage as a proxy to predict K_L vulnerability, at least in species with high leaf capacitance. Robust linear correlations between K_L decline and electrolyte leakage measurements suggested a role of membrane damage in driving leaf hydraulic collapse.

1. Introduction

Water availability is a common limiting factor for terrestrial plants growing in arid and semi-arid regions. However, global warming is expected to expose plants of several different biomes to increased risk of die-off induced by anomalous drought and heat waves (i.e., Eamus et al., 2013; Allen et al., 2015; Brodribb et al., 2019). In fact, increased air temperature and VPD are expected to exacerbate drought impacts at a global scale, even for biomes generally not water-limited (Allen et al., 2010). The impacts of species-specific die-off on biodiversity and ecosystem services are potentially dramatic, and are predicted to worsen in the next future (Anderegg et al., 2013; IPCC 2019).

Plant responses to drought are complex, and involve the coordination of different and still not well understood physiological mechanisms. There is current consensus that plant hydraulics play a critical role in setting species-specific tolerance to drought (McDowell et al., 2019). In fact, hydraulic failure has been recognized as a major correlate of drought-driven plant death (Hartmann et al., 2013; Rowland et al., 2015; Adams et al., 2017; Choat et al., 2018), and a loss of plant hydraulic conductivity (PLC) of 90% is considered a point of no return leading to plant death (Urli et al., 2013; Trifilò et al., 2015; Hammond et al., 2019). However, a number of relevant questions on correlations between hydraulic traits and plant resistance/resilience to drought remain unresolved (Cardoso et al., 2020). Most importantly, easy-to-measure and reliable indicators of drought-driven mortality risk are still largely lacking (Anderegg et al., 2019; Sapes et al., 2019; Stocker et al., 2019).

Recently, the relative water content (RWC) has been suggested as a simple indicator of plant mortality risk, due to its multiple correlations with plant hydraulics, stomatal aperture and carbon uptake (Martínez-Vilalta et al., 2019). Sapes et al. (2019) have reported good correlations between plant water content, loss of hydraulic conductivity and carbohydrate depletion in *Pinus ponderosa* samples. Stem RWC was useful for predicting loss of hydraulic conductivity in some tree species

* Corresponding author.
E-mail address: ptrifilo@unime.it (P. Trifilò).

Accepted 28 May 2021

(Rosner et al., 2019), but Mantova et al. (2021) pointed out that this might only apply to woody angiosperms, and not to conifers.

In the present study, we investigated the robustness of leaf water content as a proxy for predicting the occurrence of hydraulic failure in two native Mediterranean species, *Salvia ceratophylloides* Ard. and *Salvia officinalis* L. Climate change is expected to be exacerbated in the Mediterranean region where summer warming rates are apparently 20–40% higher than the global mean value (Mariotti et al., 2015; Lionello and Scarascia, 2018; Raymond et al., 2019). This, in turn, may affect typical biodiversity richness of the Mediterranean biome (i.e., Cowling et al., 2015; Rundel et al., 2016; Buira et al., 2021), increasing the extinction risk of different endemic species (Sala et al., 2000; Underwood et al., 2009; Cramer et al., 2018; Tramblay et al., 2020). On this view, checking possible indicators of hydraulic failure on native Mediterranean species is very relevant for improving the reliability of predictive models of Mediterranean vegetation responses to novel climate conditions.

Our study has been focused on leaf hydraulic conductance (K_L) as a major driver of plant hydraulics (Brodribb and Holbrook, 2004; Brodribb et al., 2005; Hochberg et al., 2017; Skelton et al., 2017; Scoffoni et al., 2016; Wang et al., 2018; Xiong and Nadal, 2020). Moreover, significant correlations have been reported between leaf hydraulic vulnerability and mean annual precipitation across diverse species' assemblages (Blackman et al., 2014; Nardini and Luglio, 2014), suggesting that leaf hydraulic safety plays a critical role in drought tolerance (Fang et al., 2020). Leaf hydraulic vulnerability to water stress has been originally attributed to the occurrence of xylem embolism, which was considered as the major cause of K_L decline under drought (i.e., Nardini et al., 2003; Scoffoni et al., 2011; Johnson et al., 2012). However, recent findings have outlined the relevance of the outside-xylem pathways in controlling K_L changes during dehydration (Trifilò et al., 2016, Scoffoni et al., 2017b; 2018), as well as post-drought recovery (Trifilò et al., 2020). Some studies have documented a trade-off between leaf hydraulic vulnerability and the leaf shrinkage that is typically observed during dehydration: higher shrinkage before the turgor loss point was reported for species with higher K_L vulnerability (Scoffoni et al., 2014; Trifilò et al., 2016). These results suggest that cell shrinkage might drive the K_L decline during mild dehydration by affecting the extra-xylem water transport pathway. This, in turn, may trigger stomatal closure and protect K_x from xylem embolism spread (Scoffoni et al., 2014, 2017a; Trifilò et al., 2016, 2020).

In this view, a reliable indicator of the risk of leaf hydraulic damage like leaf shrinkage (Scoffoni et al., 2014; Trifilò et al., 2016) and/or RWC thresholds (Trueba et al., 2019) may actually well quantify the risk of leaf hydraulic failure. In accordance, John et al. (2018) reported species-specific RWC thresholds for loss of leaf rehydration capacity, as a possible indicator of dehydration tolerance.

We compared the leaf hydraulic vulnerability to drought of two *Salvia* species to check if leaf water content and/or leaf shrinkage may be reliable proxies of incipient leaf hydraulic failure. We specifically tested the following hypotheses: 1) different *Salvia* species display similar critical RWC dehydration thresholds for leaf hydraulic failure; 2) leaf hydraulic failure leads to loss of leaf rehydration capacity; 3) leaf shrinkage before the turgor loss can be used as an early diagnostic tool to predict K_L impairment.

2. Materials and methods

2.1. Plant material and growth conditions

Experiments have been performed on 8-month-old plants of *S. ceratophylloides* and *S. officinalis*. *S. ceratophylloides* (*Sc*) is a rare perennial herbaceous species, endemic in southern Italy (Crisafulli et al., 2010). To the best of our knowledge, no data on hydraulics and water relations of this species are available in the literature. *S. officinalis* (*So*) is a Mediterranean-native perennial species, widely naturalized even outside its original habitat (Pignatti, 2002). Previous studies have analyzed some of the functional bases of drought tolerance of this species (Raimondo et al., 2015; Savi et al., 2016).

In October 2019, seeds provided by the Botanical garden of the University of Messina were fully immersed in water for 24 h, and then planted in greenhouse trays. After emergence of at least two developing leaves, seedlings were transferred in 3.4 L pots filled with forest topsoil collected from Colli San Rizzo (Messina, Italy). Seedlings were grown in a greenhouse until the beginning of May 2020. The greenhouse received only natural light, with maximum daily values of photosynthetic photon flux density (PPFD) averaging 810 ± 260 μmol s^{-1} m^{-2}, air temperature ranging from 21 ± 2 °C to 17 ± 2 °C (day/night), and air relative humidity of 55 ± 3%. During the growth period plants were regularly irrigated to field capacity on a daily basis. At the beginning of May, 15 samples per species were transferred in a garden of the Department CHIBIOFARAM, University of Messina. All measurements were performed in June 2020.

2.2. Pressure-volume (PV) curves and capacitance measurements

Leaf water potential at the turgor loss point (Ψ_{tlp}), osmotic potential at full turgor (π_0), bulk modulus of elasticity (ε) and leaf capacitance at full turgor were calculated based on leaf water potential isotherms measured at the beginning of June in well-watered plants. Leaves were collected from 5 different plants per species, and water potential isotherms were obtained following the procedure described by Tyree and Hammel (1972). Ψ_{tlp} was estimated as the flex point of the relationship between 1/leaf water potential (Ψ_L) and the water loss; π_0 was calculated by the y-intercept of the linear region of this relationship; ε was calculated as: $\Delta Pt/(\Delta W/W)$ where ΔPt is the change of turgor pressure and $\Delta W/W$ is the relative change of the leaf water content.

Leaf capacitance before (C_{ft}) and at Ψ_{tlp} (C_{tlp}) was estimated by PV curves analysis as well as by the fast rehydration kinetic method (FRM, Nardini et al., 2012) because *i*) differences in leaf capacitance may be obtained between different techniques (Blackman and Brodribb, 2011; Trifilò et al., 2016) and *ii*) changes in capacitance value before and at the turgor loss point have been reported in some species (Trifilò et al., 2016). On the basis of PV curves, leaf capacitance was calculated from the slope of the relationship between the water loss and Ψ_L before and after the turgor loss (i.e., $C_{ft,\,PV}$ and $C_{tlp,\,PV}$, respectively) and normalised by leaf area (A_L). Leaf images were acquired with a scanner (HP Scanjet G4050, USA) and A_L was measured with the software ImageJ (http://imagej.nih.gov/ij/). Dry weight (DW) was obtained after oven-drying leaves for 3 days at 70 °C.

For the leaf rehydration kinetic method, twelve leaves per species were cut under water and rehydrated for at least 1 h. Leaves were then dehydrated on the bench to Ψ_L values corresponding to about 50% of species-specific Ψ_{tlp} ($n = 6$), or to Ψ_{tlp} ($n = 6$). More in detail, before estimating their initial Ψ_L, samples were wrapped in plastic film, weighed to record their initial weight (W_i) and inserted in the pressure chamber to estimate their water potential. Once the balance pressure was reached, the cut section of the petiole was covered with deionized water and the pressure inside the chamber was released at a rate of 0.015 MPa s^{-1} down to atmospheric value, thus allowing leaf rehydration. At the end of pressure relaxation, the excess water was adsorbed with a filter paper and the leaf was left inside the chamber for 5 min at atmospheric pressure to allow equilibration of water content and Ψ_L. Ψ_L was measured again (i.e., final Ψ_L) and the leaf was weighed to obtain its final weight (W_f). Leaf capacitance in the turgor range ($C_{ft,FRM}$) or to Ψ_{tlp} ($C_{tlp,FRM}$) was calculated as ($W_f - W_0$)/(initial Ψ_L – final Ψ_L) and normalised by A_L.

2.3. Estimating the leaf relative water content and leaf rehydration capacity during dehydration

To check the rehydration time and avoid artefacts induced by overhydration phenomena, we measured the time course of rehydration in

both species during preliminary experiments. Ten leaves per species at different levels of dehydration were measured for their fresh weight (FW) and then rehydrated with petioles immersed in deionized water. Their weight was then measured each hour for 8 consecutive hours and 24 h later. Samples were finally oven-dried to obtain DW. The saturated water content (SWC) was reached within 5–8 h in both species and no further significant increase in leaf water content was recorded (Fig. S1B, D). For this reason, the turgid weight (TW) of measured samples was recorded after 8–12 h of rehydration.

Measurements of the relative leaf water content (RWC) and percentage loss of leaf rehydration capacity (PLRC) during dehydration were performed on samples collected from well-watered plants. Shoots were cut under water, rehydrated for about 1 h to full turgor, and bench-dehydrated for time interval ranging from 5 min to 48 h. During the rehydration and following bench-dehydration, shoots were maintained in a black plastic bag with a piece of wet filter paper inside, for at least 30 min in order to stop transpiration and favour the equilibration of water potential values across all leaves. At different dehydration levels, leaves were collected and their FW was immediately recorded. Leaves were then rehydrated for >8 h with their petiole immersed in a beaker containing deionized water, and finally oven-dried to obtain their DW. For each leaf, we calculated RWC as:

$$RWC = 100*[(FW\text{-}DW)/DW]/SWC$$

and PLRC as:

$$PLRC = 100*100\text{-}[(TW\text{-}DW)/\ DW]/SWC$$

where SWC is the saturated water content (g g^{-1}) of leaves at $\Psi_L < -0.5$ MPa. RWC is frequently estimated as: (FW-DW)/(TW-DW). However, at species-specific water content values, cells lose their rehydration ability and this produces overestimation of RWC values. In accordance, when overcoming species-specific thresholds, we recorded discrepancies between the values obtained applying the two different formulas (Supplementary Fig. 1A, C).

In order to estimate possible relationships between RWC, PLRC, leaf water potential, cell membrane damage and leaf hydraulic conductance values during the dehydration, additional leaves adjacent to those measured for RWC and PLRC, were also collected during the bench-dehydration and used for experiments described below.

Leaves measured for RWC were used also for estimating the leaf mass per unit area (LMA) (see below).

2.4. Estimating leaf hydraulic conductance changes during dehydration

Leaf hydraulic conductance (K_L) was measured using the rehydration kinetic method (RKM) (Brodribb and Holbrook, 2003). Leaves were sampled at different dehydration levels from the same shoots used for estimating RWC and PLRC (see above). One leaf was sampled and used to estimate the initial water potential (Ψ_i). A second adjacent leaf was detached with the petiole immersed in 10 mM KCl solution filtered at 0.2 μm, and left rehydrating for 30–90 s before measuring the final leaf water potential (Ψ_f). Leaf hydraulic conductance was then calculated as:

$$K_L = C*t^{-1} * \ln(\Psi_i/\Psi_f)$$

where C is the leaf capacitance, t is the rehydration time. Because differences in leaf capacitance were recorded between PV and FRM methods (see above), we used values measured by the FRM because they more closely resemble the fast water exchange occurring during leaf transpiration, opposed to slow water release during bench dehydration (Blackman and Brodribb, 2011). All K_L measurements were performed at normal laboratory irradiance (PPFD<10 μmol m^{-2} s^{-1}) and normalised at 20 °C.

2.5. Leaf hydraulic conductance response to irradiance

Light-driven changes in K_L have been recorded in different species (i.e., Scoffoni et al., 2008; Xiong et al., 2018), and in some cases can lead to changes in leaf hydraulic vulnerability (Guyot et al., 2012; Trifilò et al., 2020). To check this possible effect in our study species, measurements of K_L were performed at laboratory irradiance or after 30 min illumination by a LED light source (Dya, APOLLO LED) providing a PPFD of 1200 μmol m^{-2} s^{-1}. Measurements were performed the evaporative flux method (EFM, Sack et al., 2002). Well-watered leaves (i.e., $\Psi_L > -0.5$ MPa) were cut under water and connected to rigid peek tubing connected to a beaker containing water. The beaker rested on a digital balance and flow readings were recorded at 30s intervals at atmospheric pressure. Leaves were maintained next to a fan to promote water loss and, to avoid leaf over-heating during measurements at high irradiance, a transparent plastic container filled with water was placed between the leaf surface and the lamp.

Measurements were performed only in well-watered samples, and not repeated in dehydrating leaves because no K_L changes were recorded in response to irradiance (see Results).

2.6. Leaf cell membrane integrity

Electrolyte leakage measurements were done to obtain insights into eventual cell membrane damage induced by leaf dehydration (Trifilò et al., 2020). Measurements were performed on leaf samples collected from bench-dehydrated shoots at different dehydration levels and already used to measure RWC, PLRC, Ψ_L and K_L (see above). Leaf discs of about 0.5 cm^2 were cut with a razor blade and inserted in a test tube containing 8 mL of distilled water. Samples were stirred for 30 min at room temperature and the initial electrical conductivity of the solution (EC_i) was recorded by a conductivity meter (Cond 5, XS instruments, Italy). Samples were then subjected to three freeze-thaw cycles (i.e., T = −20 °C, +20 °C) to induce complete membrane disruption and processed as above to measure the final electrical conductivity of the solution (EC_f). The relative electrolyte leakage (REL) was calculated as (EC_i/EC_f) *100.

2.7. Minimum cuticular conductance

Minimum leaf conductance to water vapor (g_{min}) was measured in 6 leaves per species, by measuring the minimum transpiration rate divided by mole fraction vapor pressure deficit and two times the mean projected leaf area (John et al., 2018). In detail, leaves were first hydrated for >8 h. After recording their turgid weight and leaf area, they were suspended by their petioles over a fan for at least 2 h to induce stomatal closure. During this dehydration time leaves were weighed at 15 min intervals and, finally, the leaf area was measured again and leaves were oven-dried for 3 days at 70 °C to obtain DW. Room temperature and relative humidity were recorded at 30 s intervals using a thermohygrometer (Velleman, Gavere, Belgium).

2.8. Structural traits

Samples measured for RWC were used also for estimating the leaf mass per unit area (LMA) calculated as DW/A_L. Leaf shrinkage during progressive dehydration (Scoffoni et al., 2014; Trifilò et al., 2016) was measured on 15 leaves per species. Shoots were cut under water and left rehydrating for about 1 h. Fully turgid leaves were collected and immediately measured for their FW, A_L and leaf thickness (T_L, estimated by averaging values recorded in the bottom, middle, and top thirds of the leaf with a digital calliper, accuracy ± 0.01 mm). Leaf volume (V) was estimated as: $T_L \times A_L$. Samples were then fixed by their petiole to a bar opposite to a fan to favour dehydration and repeatedly measured for the above parameters at different Ψ_L values until turgor loss point was reached. They were finally oven-dried, and the above parameters were

Table 1
Mean values ± SD of leaf structural traits, water storage traits, PV traits and leaf shrinkage traits as measured in *S. ceratophylloides* and *S. officinalis* plants. Number of replicas (n) are specified and *P* values are reported. Different letters indicate statistically significant leaf capacitance values through a two-way Anova analysis (S: species, M: method, SxM: Species x Method). A_L: leaf area, V_L: leaf volume; T_L: leaf thickness; LMA: leaf mass area; SWC: leaf saturated water content; $C_{ft,\ FRKM}$ and $C_{tlp,\ FRM}$: leaf capacitance at full turgor and at turgor loss point, respectively, estimated by fast rehydration kinetic method; $C_{ft,\ PV}$ and $C_{tlp,\ PV}$: leaf capacitance at full turgor and at turgor loss point, respectively, estimated by PV curve analysis; g_{min}: minimum cuticular conductance; Ψ_{tlp}: leaf water potential at turgor loss point; π_o: osmotic potential at full turgor; ε_{max}: bulk modulus of elasticity; RWC_{tlp}: relative water content at turgor loss point; PLT_{tlp} and PLT_{dry}: percentage loss of leaf thickness at turgor loss point and of a dry leaf, respectively; PLA_{tlp} and PLA_{dry}: percentage loss of leaf area at turgor loss point and of a dry leaf, respectively; PLV_{tlp} and PLV_{dry}: percentage loss of leaf volume at turgor loss point and of a dry leaf, respectively.

	S. ceratophylloides	*S. officinalis*	*P* value
	Leaf structural	**traits**	
A_L, cm^2 ($n = 50$)	9.3 ± 4.9	17.0 ± 7.4	**<0.001**
V_L, cm^3 ($n = 15$)	0.58 ± 0.19	1.22 + 0.33	**<0.001**
T_L, mm ($n = 15$)	0.58 ± 0.08	0.79 ± 0.07	**<0.001**
LMA, g m^{-2} ($n = 50$)	55.6 ± 14.2	79.5 ± 16.5	**<0.001**
Leaf density, g cm^{-3} ($n = 15$)	0.07 ± 0.01	0.13 ± 0.02	**<0.001**
	Water storage	**traits**	
Leaf succulence, mg cm^{-2} ($n = 15$)	35.3 ± 7.9	25.2 ± 5.7	**<0.001**
SWC, g g^{-1} ($n = 7$)	5.2 ± 0.6	3.4 ± 0.3	**<0.001**
$C_{ft,\ FRM}$	0.216 ± 0.093a	0.215 ± 0.080a	**S:0.012**
mmol $m^{-2}MPa^{-1}$ ($n = 6$)			**M: <0.001**
$C_{tlp,\ FRM}$	0.667 ± 0.166 b	0.383 ± 0.078c	**SxM: 0.012**
$C_{ft,\ PV}$	2.049 ± 0.564a	1.033 ± 381.2a	**S:<0.001**
mmol $m^{-2}MPa^{-1}$ ($n = 5$)			**M: <0.001**
$C_{tlp,\ PV}$	9.941 ± 1.865b	3.984 ± 1.643c	**SxM: <0.001**
$g_{min,}$ mmol $m^{-2}s^{-1}$($n = 5$)	8.3 ± 0.5	3.2 ± 0.8	**<0.001**
	PV traits	($n = 5$)	
Ψ_{tlp} (MPa)	1.48 ± 0.04	1.87 ± 0.14	**0.02**
π_0 (MPa)	1.19 ± 0.03	1.52 ± 0.16	**0.008**
ε_{max} (MPa)	17.20 ± 3.8	27.8 ± 1.6	**<0.01**
RWC_{tlp}(%)	74.5 ± 6.9	74.70 ± 5.4	0.975
	Shrinkage traits	($n = 15$)	
PTL_{tlp}, %	21.65 ± 9.39	10.64 ± 4.56	**<0.001**
PLA_{tlp}, %	6.89 ± 2.65	6.43 ± 2.56	0.777
PLV_{tlp}, %	21.5 ± 11.5	14.07 ± 5.7	**0.005**
PTL_{dry}, %	50.20 ± 7.10	26.11 ± 7.18	**<0.001**
PLA_{dry}, %	48.54 ± 5.98	45.21 ± 4.33	0.054
PLV_{dry}, %	74.67 ± 7.98	60.86 ± 5.52	**<0.001**

measured again. The leaf water potential at different levels of dehydration was measured on leaf samples (different from those used to measure leaf shrinkage) randomly placed next to leaves used for shrinkage measurements. Two leaves for each level of dehydration were randomly selected to estimate leaf water potential (Ψ_L) with a pressure chamber (3005 Plant Water Status Console, Soilmoisture Equipment Corp., Goleta, CA, USA).

Samples measured for leaf shrinkage traits were used also to estimate leaf succulence and leaf density as:

$$\text{Leaf succulence} = SWC/A_L$$

$$\text{Leaf density} = LMA/T_L$$

2.9. Statistical analysis

To test possible differences among *Sc* and *So* in leaf structural traits, water storage traits, and data obtained by PV analysis and shrinkage traits, a *t*-test ($\alpha = 0.05$) was performed after checking for normality assumption. To test the differences among species (*Sc* and *So*) and the effects of cell turgor (i.e., before and to turgor loss point) on leaf capacitance as well as the effects of irradiance (low versus high irradiance) as measured by the EFM a two-way ANOVA test was performed. For statistically significant tests ($p < 0.05$), a Tukey's post hoc test using Holm-Sidak p-values correction was carried out to perform pairwise comparisons. Simple linear regressions were used to determine the relationships between REL to RWC, REL to Ψ_L, PLRC to REL, K_L to REL and REL to water content for each species independently. Lines were fitted for leaves with REL >15% for *Sc* and >18% for *So* (i.e., REL values recorded in well watered samples). All previous analyses were run using SigmaStat 2.0 (SPSS, Inc.,Chicago, IL, USA) statistics package. The relationship between RWC and Ψ_L, PLRC and Ψ_L, and between PLRC and RWC in each species were assessed using "fitplc" package for R software (R Core Team, 2020). Specifically, a sigmoidal model was fitted and Ψ values and associated 95% confidence intervals (C.I.s) corresponding to RWC equal to 50% (P_{RWC50}), PLRC equal to 10% and 50% (RWC_{PLRC10} and $RWC_{PLRC50,}$ respectively) and RWC values and associated 95% C.I.s corresponding to PLRC values of 10 and 50% (RWC_{PLRC10} and $RWC_{PLRC50,}$ respectively) were calculated. Using the same framework, we calculated Ψ and RWC values and associated 95% C.I.s corresponding to 10%, 50% and 88% loss of K_L in each species (P_{10}, P_{50}, P_{88}, RWC_{KL10}, RWC_{KL50}, RWC_{KL88}, respectively) as well as PLRC and associated 95% C.I.s corresponding to 10% and 50% loss of K_L in each species (i.e., $PLRC_{KL10}$ and $PLRC_{K50L}$). At last, leaf water content values and associated 95% C.I.s corresponding to PLRC of 10% and 50% and to loss of K_L of 10, 50% and 88% were also calculated. Differences of each of the abovementioned parameters between *Sc* and *So* were considered as statistically significant when the 95% C.I.s did not overlap.

3. Results

Compared to *S. ceratophylloides, S. officinalis* had higher values of leaf surface area (17 versus 10 cm^2), leaf volume (1.2 versus 0.6 cm^3), leaf thickness (0.8 versus 0.6 mm), LMA (80 versus 56 g m^{-2}) and leaf density (0.13 versus 0.07 g cm^{-3}) (Table 1). By contrast, *Sc* showed significantly higher leaf succulence (35 versus 25 mg cm^{-2}), SWC (5.2 versus 3.4 g g^{-1}) and g_{min} (8.3 ± 0.5 versus 3.2 ± 0.8 mmol m^{-2} s^{-1}) than *So*.

Leaf capacitance values before and after turgor loss, as obtained by PV curve analysis (i.e. $C_{ft,\ PV}$ and $C_{tlp,\ PV}$), were substantially higher than

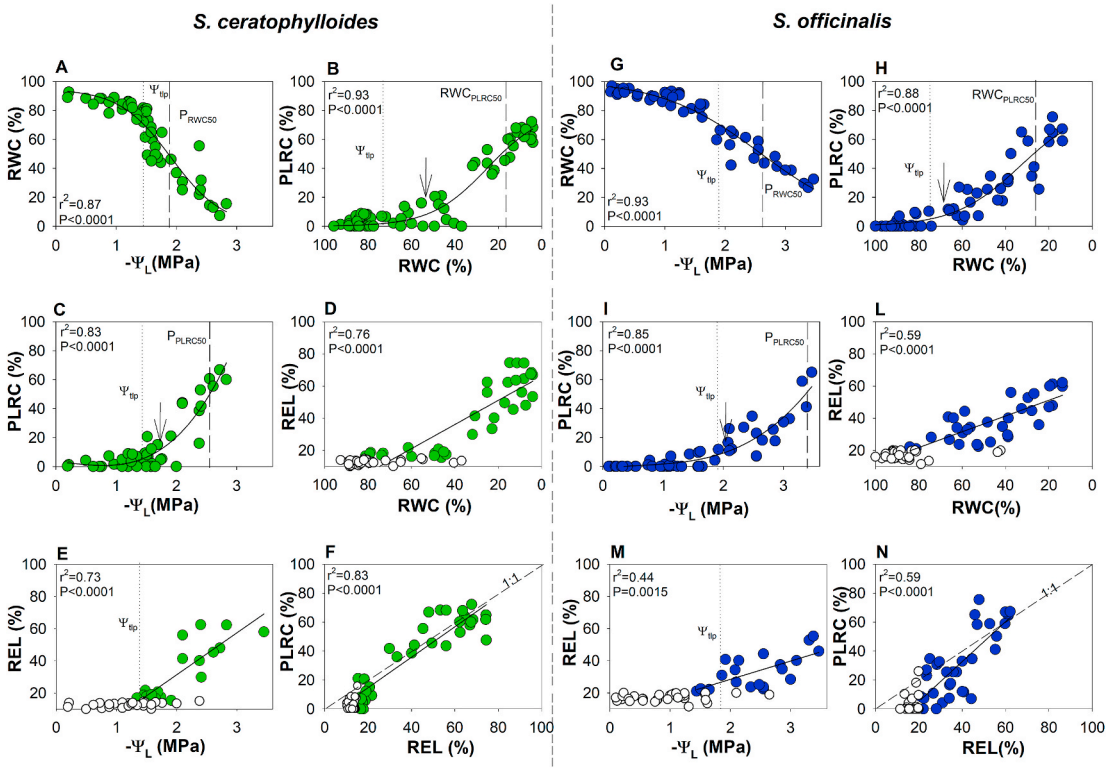

Fig. 1. Decline of relative water content RWC (**A**, **G**), percentage loss of leaf rehydration capacity PLRC (**C**, **I**) and relative electrolyte leakage REL (**E**, **M**) with decreasing leaf water potential (Ψ_L); decline of PLRC (**B**, **H**) and REL (**D**, **L**) with decreasing RWC; relationships between PLRC and REL (**F**, **N**) as measured in *S. ceratophylloides* (green circles) and *S. officinalis* (blue circles). Best fitted regression curves are designed by dark line. White symbols indicate data not included in the regression. Fitted regression are as follows: A): RWC = 94.83/(1 + exp(-(Ψ_L-1.91)/-0.43)); B): PLRC = 80.6/(1 + exp(-(RWC-24.99)/-13)); C) PLRC = 3.5–4.43*Ψ_L-2.37* Ψ_L^2+4.4* Ψ_L^3; D) REL = 66.1–0.75*RWC; E) REL = −20.8 + 26.1 * Ψ_L; F) PLRC: = −6.3 + 1.05*REL; G) RWC = 101.2/(1 + exp(-(Ψ_L -2.58)/-0.83)); H) PLRC = 83.57/(1 + exp(-(RWC-33.14)/-15.1)); I) PLRC = −1.3 + 4.81* Ψ_L -3.95* Ψ_L^2+2.1* Ψ_L^3; L) REL = 60.9–0.49*RWC; M) REL = 5.6 + 11.4*Ψ_L; N) PLRC = −22.45 + 1.38*REL. r^2 and *P* value of each regression are reported. Dotted lines indicate the leaf water potential at turgor loss point (Ψ_{tlp}). Arrows in B), C), H), I) indicate the PLRC thresholds. Long dashed lines in B) and H) indicate the RWC value inducing 50% PLRC (RWC_{PLRC50}). Long dashed lines in C) and I) indicate the Ψ_L value inducing 50% PLRC (P_{PLRC50}). Short dashed lines in F) and N) indicate the 1:1 relationship. (For interpretation of the references to colour in this figure legend, the reader is referred to the Web version of this article.)

values obtained by the fast rehydration kinetic method (i.e. $C_{ft,FRM}$ $C_{tlp,FRM}$, Table 1). Nevertheless, the two techniques showed a similar trend, in that leaf capacitance was similar in the two species, independent on the method (i.e., about 0.22 mol $m^{-2}s^{-1}$ MPa^{-1} by FRM and about 1.5 mol $m^{-2}s^{-1}$ MPa^{-1} by PV curve analysis). An increase in leaf capacitance was recorded at the turgor loss point in both species and by both methods (Table 1). It can be noted that at the turgor loss point, *Sc* showed values of leaf capacitance about 2 times higher than *So* (i.e., 0.67 versus 0.38 mol m^{-2} MPa^{-1} by FRM and 9.9 versus 4 mol m^{-2} MPa^{-1} by PV analysis, respectively).

So showed significantly lower Ψ_{tlp} (−1.9 versus −1.5 MPa) and π_o (−1.5 versus −1.2 MPa), and higher ε_{max} (28 versus 17 MPa) compared to *Sc*, but similar RWC_{tlp} values were recorded in the two species.

At turgor loss point and in dry leaf samples, the percentage loss of leaf thickness and leaf volume were significantly higher in *Sc* compared to *So* (Table 1), while no significant difference in percentage loss of leaf area (PLA) value was recorded.

The two study species showed an increase in PLRC and relative electrolyte leakage (REL) in response to dehydration (i.e., at more negative Ψ_L and lower RWC values, Fig. 1). However, the RWC values inducing 10% loss of rehydration capacity (i.e., RWC_{PLRC10}), taken as a proxy of critical dehydration threshold (John et al., 2018), were different in the two species. In fact, RWC_{PLRC10} was about 55% in *S. ceratophylloides* and about 70% in *S. officinalis* (Fig. 1B, H, Supplementary Table 1). Moreover, differences were recorded also in terms of RWC values inducing 50% loss of rehydration capability (RWC_{PLRC50}). This parameter was about 17% in *Sc* and 27% in *So* (Fig. 1B, H, Supplementary Table S1). Differences in Ψ_L values inducing 10% and 50% loss of rehydration capacity were recorded in *Sc* and *So* too (Fig. 1C, I, Supplementary Table S1). The increase in PLRC during dehydration was likely induced by increasing cell membrane damage, as positive correlations between PLRC and REL were recorded in both species (Fig. 1F, N). It can be noted that an increase in REL in response to dehydration occurred at similar Ψ_L values (about −1.3 MPa, Fig. 1E, M) but at different relative water content (i.e., RWC ~ 70% and 85% in in *Sc* and *So*, respectively, Fig. 1D, L).

Irradiance did not affect K_L in the two species (Table 2). *Sc* and *So* showed a similar leaf hydraulic vulnerability in response to dehydration if Ψ_L values were taken into account (Fig. 2A, E, Supplementary Table 1). In fact, similar water potential value inducing 50% and 88% loss of K_L was recorded in the two *Salvia* species (i.e., P_{50} ~ −2.0 MPa,

Table 2
Mean values ± SD ($n = 5$) of leaf hydraulic conductance (K_L) as measured in the two *Salvia* species at low and high irradiance (LI and HI, respectively) by the evaporative flux method (EFM). *P* values as result of a two-way ANOVA by species (S), and irradiance (I) are given.

	S. ceratophylloides K_L (mmol $m^{-1}s^{-1}MPa^{-1}$)		*S. officinalis* K_L (mmol $m^{-1}s^{-1}MPa^{-1}$)		*P* value
	LI	HI	LI	HI	
EFM	21.7 ± 2.8	20.9 ± 6.1	17.9 ± 1.9	16.9 ± 2.3	**S: 0.045** I: 0.871 SxM: 0.987

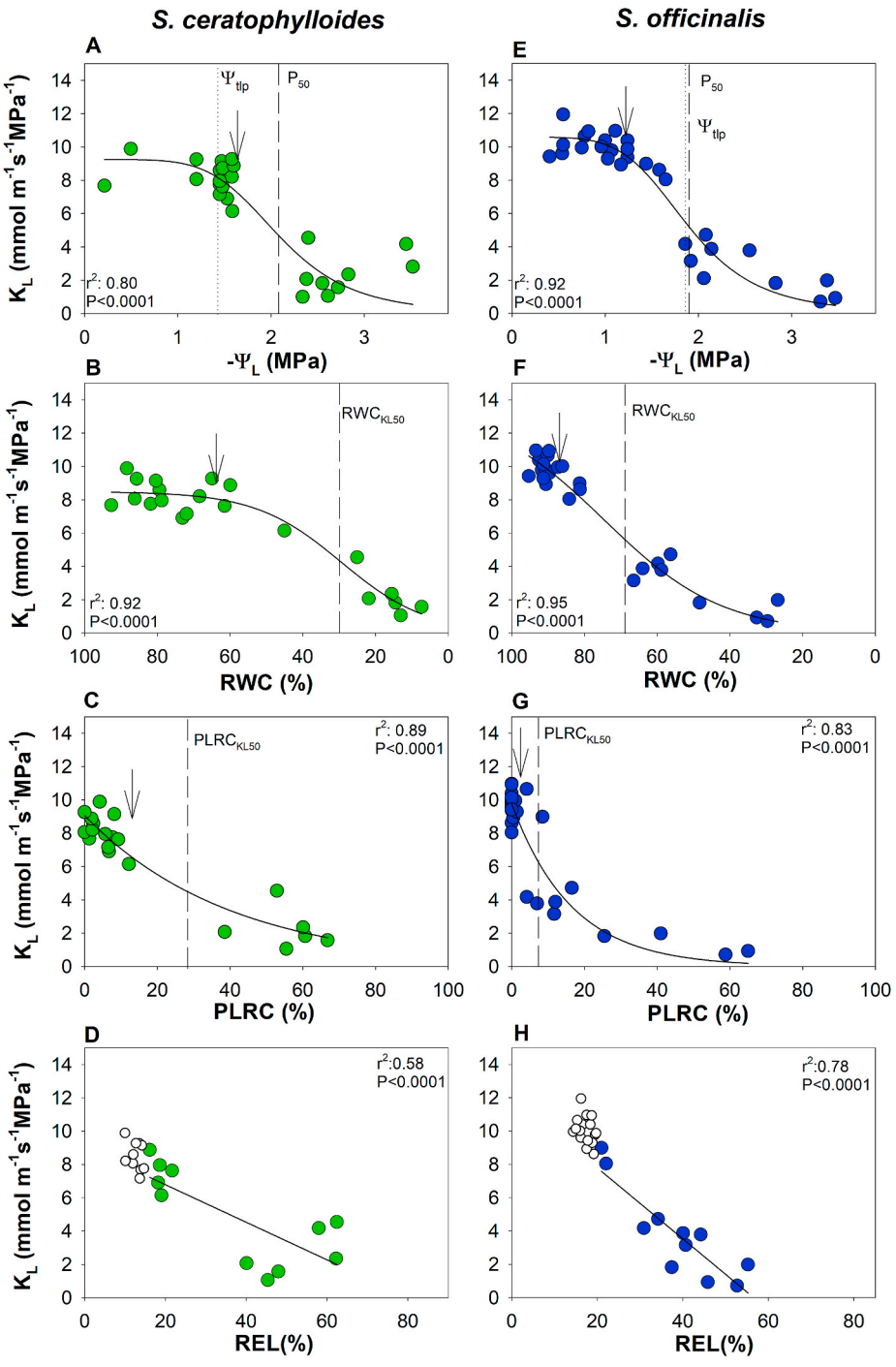

Fig. 2. Decline of leaf hydraulic conductance (K_L) as a function of the leaf water potential Ψ_L (**A**, **E**), and the relative water content (**B**, **F**); relationships between K_L and percentage loss of leaf rehydration capacity PLRC (**C**, **G**) and relative electrolyte leakage REL (**D**, **H**) as measured in *S. ceratophylloides* (green circles) and *S. officinalis* (blue circles). Best fitted regression curve is designed by dark line. White symbols indicate values not included in the regression. Fitted regression are as follows: A) $K_L = 9.24/[1 + (\Psi_L/2.09)^{5.29}]$; B) $K_L = 8.5/(1 + \exp(-(RWC-29.4)/11.9))$; C) $K_L = 9.05*\exp(-0.02*PLRC)$; D) $K_L = 9.04–0.11*REL$; E) $K_L = 10.6/[1 + (\Psi_L/1.88)^{4.98}]$; F) $K_L = 13.6/(1 + \exp(-(RWC-74.6)/16.3))$; G) $K_L = 9.77*\exp(-0.06*PLRC)$; H) $K_L = 12.05–0.21*REL$. r^2 and *P* value of each regression are reported. Dotted lines indicate the leaf water potential at turgor loss point (Ψ_{tlp}). Arrows in A), B), E), F) indicate K_L thresholds. Long dashed lines in A) and E) indicate the Ψ_L value inducing 50% loss of K_L (P_{50}), in B) and F) indicate the RWC value inducing 50% loss of K_L (RWC_{KL50}) and in C) and G) indicate the PLRC value inducing 50% loss of K_L ($PLRC_{KL50}$). (For interpretation of the references to colour in this figure legend, the reader is referred to the Web version of this article.)

$P_{88} \sim -3.2$ MPa, Fig. 2A, E, Supplementary Table 1). By contrast, values of RWC inducing 50% and 88% loss of K_L (i.e., RWC_{KL50} and RWC_{KL50}, respectively) were different. In particular, RWC_{KL50} was about 35% for *S. ceratophylloides* and 65% for S. *officinalis* and RWC_{KL88} was about 15% for *S. ceratophylloides* and 40% for S. *officinalis* (Fig. 2B, F, Supplementary Table 1). A 50% loss of K_L was recorded at different PLRC values ($PLRC_{KL50}$). The $PLRC_{KL50}$ was about 30% in *Sc* and 10% in *So* (Fig. 2C, G, Supplementary Table 1). Moreover, a tight correlation between K_L and REL was recorded in both species (Fig. 2D, H).

The study species showed different leaf saturated water content, i.e., 5.2 ± 0.6 g g^{-1} in *Sc* versus 3.4 ± 0.3 g g^{-1} in *So* (Table 1). This difference led to leaf hydraulic impairment occurring at different RWC but at similar absolute water content values (Fig. 3). Indeed, the increase in REL occurred at a leaf water content of about 2.9 g g^{-1} and, even more surprisingly, the most commonly used hydraulic conductance loss thresholds (i.e., 10%, 50% and 88% loss of K_L) were recorded at the same water content in *Sc* versus *So* (i.e., about 2.9 g g^{-1}, 1.8 g g^{-1} and 1.3 g g^{-1}, respectively, Fig. 3, Supplementary Table 1).

4. Discussion

Our data reveal that similar leaf water content thresholds induce similar leaf hydraulic impairment in two *Salvia* species, suggesting that leaf water content (but not RWC) might be a useful warning proxy for leaf hydraulic failure. Indeed, in contrast to our working hypothesis, *Sc* and *So* showed different RWC thresholds for leaf hydraulic failure, but

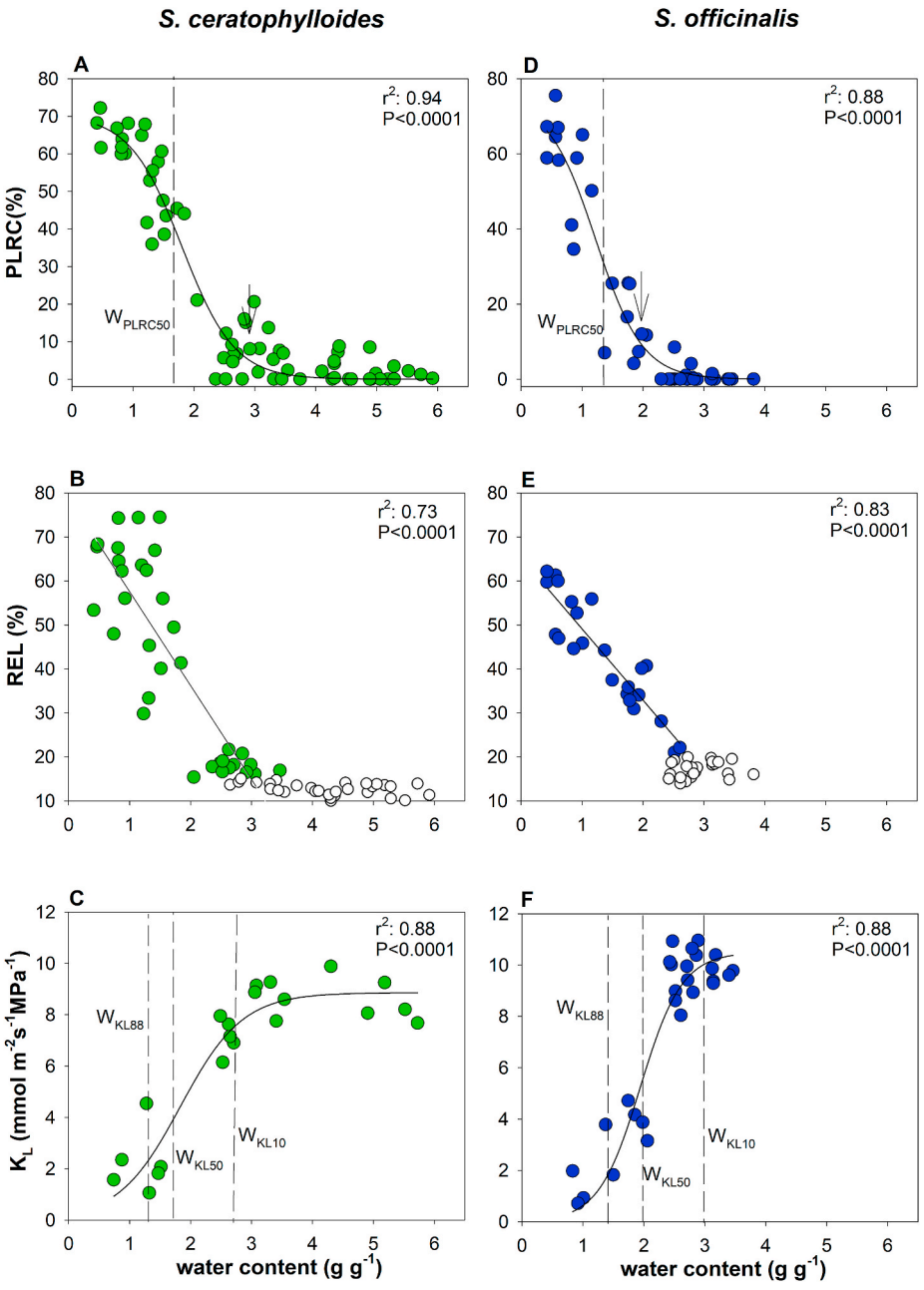

Fig. 3. Relationships between water content (W) and percentage loss of leaf rehydration capacity, PLRC (**A**, **D**), relative electrolyte leakage, REL (**B**, **E**) and leaf hydraulic conductance K_L (**C**, **F**) as measured in *S. ceratophylloides* (green circles) and *S. officinalis* (blue circles). Best fitted regression curve is designed by dark line. White symbols indicate not included in the regression. Fitted regression are as follows: A) PLRC = 68.3/(1 + exp(-(W-2.04)/-0.41)); B) REL = 78.9–21.4*W; C) K_L = 8.8/(1 + exp(-(W-1.8)/0.5)); D) PLRC = 74.3/(1 + exp(-(W-1.22)/-0.38)); E) REL = 65.3–16.2*W; F) K_L = 10.5/(1 + exp(-(W-1.9)/0.34)). r^2 and *P* value of each regression are reported. Arrows in A) and D) indicate PLRC thresholds. Long dashed lines in A) and D) indicate the water content inducing 50% loss of PLRC value (W_{PLRC50}), in C) and F) indicate the water content value inducing 10% (W_{KL10}), 50% (W_{KL50}) and 88 (W_{KL88}) loss of K_L. (For interpretation of the references to colour in this figure legend, the reader is referred to the Web version of this article.)

similar leaf water content values leading to leaf hydraulic decline during dehydration and cell membrane damage. Moreover, the lack of any K_L decline until the turgor loss point in *Sc*, despite consistent leaf shrinkage, provide new insights into the relations between leaf shrinkage and leaf hydraulic vulnerability. In fact, this result and the tight and linear correlation between K_L impairment and REL as recorded in *Sc* and *So,* strongly suggest that K_L decline is driven by leaf cell membrane damages, regardless of the amount of leaf shrinkage. Thus, leaf shrinkage alone does not always predict K_{ox} impairment, as previous studies had suggested (Trifilò et al., 2016; Scoffoni et al., 2017a). In this view, cell membrane damage, but not leaf shrinkage, may offer a more useful tool for monitoring the risk of K_L decline under drought.

4.1. Leaf water storage and its relationships with leaf hydraulic vulnerability

Sc and *So* showed different water-use strategies, as indicated by significantly different leaf water relation parameters. In *Sc*, the relatively low modulus of elasticity, coupled to high SWC and leaf capacitance, allowed maintaining relatively high cell water content during the first steps of dehydration with respect to *So*. This behaviour apparently delayed leaf hydraulic impairment caused by turgor loss. After the turgor loss point, the increase in leaf capacitance recorded in *Sc* increased the water loss per unit change in water potential, thus inducing a more rapid drop in RWC compared to *So*. Water relations of *So* have been described in previous studies, highlighting the drought tolerance strategy of the species (Raimondo et al., 2015; Savi et al., 2016). Lower Ψ_{tlp} and π_o values, and higher bulk ε_{max} of *So* compared to *Sc*, would confirm such a drought tolerance strategy (Bartlett et al., 2012; Tombesi et al., 2014). It should be noted that higher cell wall rigidity causes sharper drop of Ψ_L per unit water loss (i.e., Tyree and Hammel, 1972; Bartlett et al., 2012), leading to higher RWC_{tlp} (Salleo, 1983). However, likely because of similar values of leaf capacitance before the turgor loss and about 0.4 MPa lower Ψ_{tlp} as recorded in *So*

versus *Sc*, the RWC_{tlp} was similar in the two species. These contrasting water use strategies are consistent with recorded differences in terms of leaf succulence, which was higher in *Sc* compared to *So*. Moreover, differences between the two species were recorded in terms of leaf capacitance at the turgor loss point: it was two-fold higher in *Sc* than in *So*. Succulence syndrome is common for species living in semi-arid habitats, where the occurrence of dry periods is balanced by rain events and water inputs from fog or dew that can supplement the low precipitations (Ogburn and Edwards, 2010; Griffiths and Males, 2017). High water storage allows plants to maintain relatively stable leaf water potential and water content despite fluctuations of transpiration rate and water supply (Sack and Tyree, 2005). Thus, succulence allows avoiding drought damage at the cellular level and maintaining, as long as possible, metabolic activity (Eggli and Nyffeler, 2009; Ogburn and Edwards, 2010; Griffiths and Males, 2017; Males, 2017). However, no sharp distinction exists between succulent and non-succulent species and, for this reason, succulence is considered as a "continuous" trait (Ogburn and Edwards, 2010; Griffiths and Males, 2017). This was also the case for the two *Salvia* species, with *So* showing a moderate succulence syndrome as well. In fact, *So* showed lower cuticular transpiration and higher V_L and T_L than *Sc,* and similarly high values of leaf capacitance before the turgor loss were recorded in *Sc* and *So* (Pivovaroff et al., 2014). Moreover, large parenchymatic cells without chloroplasts were observed around veins of the two study species (data not shown). These cells, observed also in other *Salvia* species (i.e., Kahraman et al., 2010; Erbano et al., 2012; Bercu et al., 2012), can exhibit high water retention efficiency and might be involved in water storage (Muries et al., 2019).

Different hydraulic behaviour between the two species emerged also in terms of K_L responses to dehydration. In *Sc*, K_L decline only occurred after the turgor loss point and at RWC values as low as about 65%. Similarly, an increase in PLRC was recorded at $\Psi_L < \Psi_{tlp}$ and at RWC of about 55%. By contrast, in *So* the K_L decline started before the turgor loss point (i.e., P_{10} occurred at $\Psi_L < -1.3$ MPa) and at RWC of about 90%. Moreover, loss of rehydration ability occurred at $\Psi_L \sim \Psi_{tlp}$ and at RWC values as high as about 70%, already. Hence, different RWC thresholds were indicative of leaf hydraulic decline in *Sc* versus *So*. Surprisingly, thresholds of leaf hydraulic vulnerability corresponded to very similar absolute leaf water content in *Sc* and *So*. In fact, due to different leaf SWC in the two species, 10%, 50% and 88% loss of K_L occurred at different leaf water potential and RWC, but at similar absolute water content. Water content values approaching 3 g g^{-1} (corresponding to RWC values of about 60% in *Sc* and 85% in *So*) triggered leaf membrane damage in both species, strongly affecting K_L (see also comments below). In summary, higher SWC and succulence allowed *Sc* to maintain sufficiently high water content to delay hydraulic impairment under water deprivation and down to turgor loss point. Moreover, the critical leaf water content of 3 g g^{-1} induced a rapid increase in membrane and hydraulic damage (as recorded in terms of PLRC, REL and K_L) also in this species, as observed for *So*.

It can be noted that not only absolute leaf water content but also Ψ_L resulted a useful proxy to monitor the risk of hydraulic impairment. Ψ_L values of about −2 MPa induced 50% loss of K_L as well as Ψ_L values of about −1.3 MPa caused initial increase in leaf cell membrane damages. Actually, leaf water content and Ψ_L changes during dehydration provide different indicators of leaf hydraulic impairment during dehydration. Water content changes likely better convey the loss in cell volume and then cell membranes damage. Thus, it can better explain damages at cell level. By contrast, because Ψ_L thresholds vary enormously among species (Bartlett et al., 2012; Trueba et al., 2019) it may be particularly useful for monitoring drought-induced mortality at intra-specific (Sapes and Sala, 2020) or, as in the present study, at interspecific level.

4.2. Role of the extra-xylem pathway, and of cell membrane integrity, in governing K_L decline during dehydration

Leaf hydraulic conductance depends on the features of both xylem (K_x) and extra-xylem (K_{ox}) water pathways. During dehydration, the xylem pathway can be compromised by xylem embolism events that, in turn, are triggered when species-specific water potential values are surpassed (i.e., Sack and Scoffoni, 2013; Petruzzellis et al., 2020). K_{ox} decline is putatively caused by different mechanisms related to alterations in cell turgor and in cell membrane permeability and/or integrity, loss in cell-to-cell connectivity and changes in the leaf evaporation sites (Buckley, 2015). Indeed, our data confirm that turgor loss point is a critical threshold for leaf hydraulic impairment of the two *Salvia* species (Bartlett et al., 2012; Scoffoni et al., 2014; Trueba et al., 2019). In fact, it represented the threshold of leaf hydraulic decline for *Sc* and the value at which 50% loss of hydraulic conductance was recorded in *So*.

Higher shrinkage was recorded in *Sc* compared to *So*, i.e., in the species with lower ε_{max} and higher Ψ_{tlp}. However, in *Sc* no K_L (and likely K_{ox}) decline occurred until Ψ_{tlp}, despite ongoing leaf shrinkage, suggesting that leaf shrinkage per se does not always affect K_{ox}. This result is in contrast with some previous studies reporting relationships between leaf shrinkage and drought tolerance traits (as Ψ_{tlp}, π_0, ε and LMA) and suggesting that leaf shrinkage may drive leaf hydraulic decline during mild dehydration (Scoffoni et al., 2014). Despite leaf shrinkage, membrane integrity was preserved down to water potential approaching Ψ_{tlp}, i.e., at Ψ_L causing already about 10% and 50% loss of K_L in *Sc* and *So,* respectively. These results suggest that leaf shrinkage, at least during the first steps of dehydration, did not cause any loss in membrane integrity, although it might have affected membrane water permeability, especially where a parallel K_{ox} decline was recorded. Only above species-specific thresholds, severe cell shrinkage would cause membrane damage leading to hydraulic decline. Thus, even relevant leaf shrinkage, as long as membrane integrity is maintained, would not cause irreversible leaf hydraulic dysfunction (Scoffoni et al., 2014; Trifilò et al., 2020).

4.3. Conclusion

Our study shows that absolute leaf water content, but not RWC, is a reliable proxy of species-specific risk of irreversible hydraulic damage. In fact, despite the robust correlations between RWC and leaf membrane damage, K_L and PLRC as recorded in *Sc* as well as in *So,* no statistically similar RWC threshold inducing leaf hydraulic impairment was recorded in *Sc* and *So*. By contrast, similar leaf absolute water content values induced similar leaf hydraulic damages. Future investigations on a higher number of species and, mainly, on the effects of the leaf water content on whole plant fitness are needed to confirm our findings.

The loss in membrane integrity that occurred independently on the amount of leaf shrinkage had a key role in driving K_L decline, likely causing K_{ox} failure. Moreover, the recorded cell membrane drought resistance thresholds for hydraulic impairment suggest that changes in leaf cell vitality (easily measurable via electrolyte leakage tests) may be a very useful tool for monitoring the risk of irreversible leaf hydraulic failure. By contrast, leaf shrinkage may be a poor indicator of dehydration-induced damage, especially when species with significant succulence syndromes are considered.

Contribution

PT, EA and AN conceived and designed the experiments. EA and PT performed the measurements and analyzed the data. FP performed the statistical analysis. PT and AN wrote the manuscript, with contributions by all co-Authors. All Authors read and approved.

Declaration of competing interest

The Authors declare that they have no known competing financial interests or personal relationships that could have appeared to influence the work reported in this paper.

Aknowledgements

This study was supported by Ministero dell'Istruzione, dell'Università e della Ricerca, Grant/Award Number: FFABR 2017.

Appendix A. Supplementary data

Supplementary data to this article can be found online at https://doi.org/10.1016/j.plaphy.2021.05.046.

References

Adams, H.D., Zeppel, M.J., Anderegg, W.R., et al., 2017. A multispecies synthesis of physiological mechanisms in drought-induced tree mortality. Nat. Ecol. Evol. 1, 1285–1291.

Allen, C.D., Macalady, A.K., Chenchouni, H., et al., 2010. A global overview of drought and heat-induced tree mortality reveals emerging climate change risks for forests. For. Ec. Man. 259, 660–684.

Allen, C.D., Breshears, D.D., Mcdowell, N.G., 2015. On underestimation of global vulnerability to tree mortality and forest die-off from hotter drought in the Anthropocene. Ecosphere 6, art129.

Anderegg, W.R.L., Kane, J.M., Anderegg, L.D.L., 2013. Consequences of widespread tree mortality triggered by drought and temperature stress. Nat. Clim. Change 3, 30–36.

Anderegg, W.R.L., Anderegg, L.D.L., Kerr, K.L., Trugman, A.T., 2019. Widespread drought-induced tree mortality at dry range edges indicates that climate stress exceeds species' compensating mechanisms. Global Change Biol. 25, 3793–3802.

Bartlett, M.K., Scoffoni, C., Sack, L., 2012. The determinants of leaf turgor loss point and prediction of drought tolerance of species and biomes: a global meta-analysis. Ecol. Lett. 15, 393–405.

Bercu, R., Negrean, G., Broască, L., 2012. Leaf anatomical study of taxons *Salvia nemorosa* subsp. tesquicola, *Salvia nutans*, and *Salvia* × *Sobrogensis* from Dobrudja. Bot. serb. 36, 103–109.

Blackman, C.J., Brodribb, T.J., 2011. Two measures of leaf capacitance: insights into the water transport pathway and hydraulic conductance in leaves. Funct. Plant Biol. 38, 118–126.

Blackman, C.J., Gleason, S.M., Chang, Y., Cook, A.M., Laws, C., Westob, M., 2014. Leaf hydraulic vulnerability to drought is linked to site water availability across a broad range of species and climates. An. Bot. 114, 435–440.

Brodribb, T.J., Holbrook, N.M., 2003. Stomatal closure during leaf dehydration, correlation with other leaf physiological traits. Plant Physiol. 132, 2166–2173.

Brodribb, T.J., Holbrook, N.M., 2004. Stomatal protection against hydraulic failure: a comparison of coexisting ferns and angiosperms. New Phytol. 162, 663–670.

Brodribb, T.J., Holbrook, N.M., Zwieniecki, M.A., Palma, B., 2005. Leaf hydraulic capacity in ferns, conifers and angiosperms: impacts on photosynthetic maxima. New Phytol. 165, 839–846.

Brodribb, T.J., Cochard, H., Rodriguez Dominguez, C., 2019. Measuring the pulse of trees; using the vascular system to predict tree mortality in the 21st century. Conserv. Physiol. 7, coz046.

Buckley, T.N., 2015. The contributions of apoplastic, symplastic and gas phase pathways for water transport outside the bundle sheath in leaves. Plant Cell Environ. 38, 7–22.

Buira, A., Fernández-Mazuecos, M., Aedo, C., Molina-Venegas, R., 2021. The contribution of the edaphic factor as a driver of recent plant diversification in a Mediterranean biodiversity hotspot. J. Ecol. 109, 987–999.

Cardoso, A.A., Billon, L.M., Borges, A.F., Fernandez-de-Una, L., Gersony, J.T., Guney, A., Johnson, K.M., Lemaire, C., Mrad, A., Wagner, Y., Petit, G., 2020. New developments in understanding plant water transport under drought stress. New Phytol. 227, 1025–1027.

Choat, B., Brodribb, T.J., Brodersen, C.R., Duursma, R.A., Lopez, R., Medlyn, B.E., 2018. Triggers of tree mortality under drought. Nature 558, 531–539.

Cowling, R.M., Potts, A.J., Bradshaw, P., et al., 2015. Variation in plant diversity in Mediterranean climate ecosystems: the role of climatic and topographical stability. J. Biogeogr. 42, 552–564.

Cramer, W., Guiot, J., Fader, M., et al., 2018. Climate change and interconnected risks to sustainable development in the Mediterranean. Nat. Clim. Change 8, 972–980.

Crisafulli, A., Cannavò, S., Maiorca, G., Musarella, C.M., Signorino, G., Spampinato, G., 2010. Aggiornamenti floristici per la Calabria. Inf. Bot. Ital. 42, 437–448.

Eamus, D., Boulain, N., Cleverly, J., Breshears, D.D., 2013. Global change-type drought-induced tree mortality: vapor pressure deficit is more important than temperature per se in causing decline in tree health. Ecol. Evol. 3, 2711–2729.

Eggli, U., Nyffeler, R., 2009. Living under temporarily arid conditions-succulence as an adaptive strategy. Bradleya 27, 13–36.

Erbano, M., Ehrenfried, A.S.L., Pereira Dos Santos, L., 2012. Morphoanatomical and phytochemical studies of *Salvia lachnostachys* (Lamiaceae). Microsc. Res. Tech. 75, 1737–1744.

Fang, J., Lutz, J.A., Wang, L., Shugart, H.H., Yan, X., 2020. Using climate-driven leaf phenology and growth to improve predictions of gross primary productivity in North American forests. Global Change Biol. 26, 6974–6988.

Griffiths, H., Males, J., 2017. Succulent plants. Curr. Biol. 27, R890–R896.

Guyot, G., Scoffoni, C., Sack, L., 2012. Combined impacts of irradiance and dehydration on leaf hydraulic conductance: insights into vulnerability and stomatal control. Plant Cell Environ. 35, 857–871.

Hammond, W.M., Yu, K., Wilson, L.A., Will, R.E., Anderegg, W.R.L., Adams, H.D., 2019. Dead or dying? Quantifying the point of no return from hydraulic failure in drought-induced tree mortality. New Phytol. 223, 1834–1843.

Hartmann, H., Ziegler, W., Kolle, O., Trumbore, S., 2013. Thirst beats hunger – declining hydration during drought prevents carbon starvation in Norway spruce saplings. New Phytol. 200, 340–349.

Hochberg, U., Windt, C.W., Ponomarenko, A., Zhang, Y.J., Gersony, J., Rockwell, F.E., Holbrook, N.M., 2017. Stomatal closure, basal leaf embolism and shedding protect the hydraulic integrity of grape stems. Plant Physiol. 174, 764–775.

IPCC, 2019. In: Shukla, P.R., Skea, J., Calvo Buendia, E., Masson-Delmotte, V., Pörtner, H.O., Roberts, D.C., Zhai, P., Slade, R., Connors, S., van Diemen, R., Ferrat, M., Haughey, E., Luz, S., Neogi, S., Pathak, M., Petzold, J., Portugal Pereira, J., Vyas, P., Huntley, E., Kissick, K., Belkacemi, M., Malley, J. (Eds.), Climate Change and Land: an IPCC Special Report on Climate Change, Desertification, Land Degradation, Sustainable Land Management, Food Security, and Greenhouse Gas Fluxes in Terrestrial Ecosystems.

John, G.P., Henry, C., Sack, L., 2018. Leaf rehydration capacity: associations with other indices of drought tolerance and environment. Plant Cell Environ. 41, 2638–2653.

Johnson, D.M., McCulloh, K.A., Meinzer, F.C., Woodruff, D.R., 2012. Evidence for leaf xylem embolism as a primary factor in dehydration induced declines in leaf hydraulic conductance. Plant Cell Environ. 35, 760–769.

Kahraman, A., Celep, F., Dogan, M., 2010. Anatomy, trichome morphology and palynology of *Salvia chrysophylla* Stapf (Lamiaceae). South Afr. J. Bot. 76, 187–195.

Lionello, P., Scarascia, L., 2018. The relation between climate change in the Mediterranean region and global warming. Reg. Environ. Change 18, 1481–1493.

Males, J., 2017. Secrets of succulence. J. Exp. Bot. 9, 2121–2134.

Mantova, M., Menezes-Silva, P.E., Badel, E., Cochard, H., 2021. The interplay of hydraulic failure and cell vitality explains tree capacity to recover from drought. Physiol. Plantarum. https://doi.org/10.1111/ppl.13331.

Mariotti, A., Pan, Y., Zeng, N., Alessandri, A., 2015. Long-term climate change in the Mediterranean region in the midst of decadal variability. Clim. Dynam. 44, 1437–1456.

Martínez-Vilalta, J., Anderegg, W.R., Sapes, G., Sala, A., 2019. Greater focus on water pools may improve our ability to understand and anticipate drought-induced mortality in plants. New Phytol. 223, 22–32.

McDowell, N.G., Brodribb, T.J., Nardini, A., 2019. Hydraulics in the 21st Century New Phytol, vol. 224, pp. 537–542.

Muries, B., Mom, R., Benoit, P., et al., 2019. Aquaporins and water control in drought-stressed poplar leaves: a glimpse into the extra-xylem vascular territories. Environ. Exp. Bot. 162, 25-3.

Nardini, A., Luglio, J., 2014. Leaf hydraulic capacity and drought vulnerability: possible trade-offs and correlations with climate across three major biomes. Funct. Ecol. 28, 810–818.

Nardini, A., Salleo, S., Raimondo, F., 2003. Changes in leaf hydraulic conductance correlate with leaf vein embolism in. *Cercis siliquastrum* L. Trees 17, 529–534.

Nardini, A., Pedà, G., Salleo, S., 2012. Alternative methods for scaling leaf hydraulic conductance offer new insights into the structure-function relationships of sun and shade leaves. Funct. Plant Biol. 39, 394–401.

Ogburn, R.M., Edwards, E.J., 2010. The ecological water-use strategies of succulent plants. In: Kader, J.C., Delseny, M. (Eds.), Advances in Botanical Research, vol. 55. Academic Press, Burlington, MA, pp. 179–225.

Petruzzellis, F., Tomasella, M., Miotto, A., Natale, S., Trifilò, P., Nardini, A., 2020. A Leaf Selfie: using a smartphone to quantify leaf vulnerability to hydraulic dysfunction. Plants 9, 234.

Pignatti, S., 2002. Flora d'Italia. Edagricole.

Pivovaroff, A.L., Sack, L., Santiago, L.S., 2014. Coordination of stem and leaf hydraulic conductance in southern California shrubs: a test of the hydraulic segmentation hypothesis. New Phytol. 203, 842–850.

Raimondo, F., Trifilò, P., Lo Gullo, M.A., Andri, S., Savi, T., Nardini, A., 2015. Plant performance on Mediterranean green roofs: interaction of speciesspecific hydraulic strategies and substrate water relations. AoB Plants 7, plv007.

Raymond, F., Ullmann, A., Tramblay, Y., Drobinski, P., Camberlin, P., 2019. Evolution of Mediterranean extreme dry spells during the wet season under climate change. Reg. Environ. Change 19, 2339–2351.

Rosner, S., Heinze, B., Savi, T., Dalla-Salda, G., 2019. Prediction of hydraulic conductivity loss from relative water loss: new insights into water storage of tree stems and branches. Physiol. Plantarum 165, 843–854.

Rowland, L., da Costa, A.C.L., Galbraith, D.R., Oliveira, R., Binks, O.J., Oliveira, A., Pullen, A., Doughty, C., Metcalfe, D., Vasconcelos, S., 2015. Death from drought in tropical forests is triggered by hydraulics not carbon starvation. Nature 528, 119.

Rundel, P.W., Arroyo, M.T.K., Cowling, R.M., Keeley, J.E., Lamont, B.B., Vargas, P., 2016. Mediterranean biomes: evolution of their vegetation, floras, and climate. Annu. Rev. Ecol. Evol. Syst. 47, 383–407.

Sack, L., Scoffoni, C., 2013. Leaf venation: structure, function, development, evolution, ecology and applications in the past, present and future. New Phytol. 198, 983–1000.

Sack, L., Tyree, M.T., 2005. Leaf hydraulics and its implications in plant structure and function. In: Holbrook, N.M., Zweiniecki, M.A. (Eds.), Vascular Transport in Plants. Elsevier Academic Press, Oxford, UK.

Sack, L., Melcher, P.J., Zwieniecki, M.A., Holbrook, N.M., 2002. The hydraulic conductance of the angiosperm leaf lamina: a comparison of three measurement methods. J. Exp. Bot. 53, 2177–2184.

Sala, O.S., Stuart Chapin III, F., Armesto, J.J., et al., 2000. Global biodiversity scenarios for the year 2100. Science 287, 1770–1774.

Salleo, S., 1983. Water relations parameters of two Sicilian species of Senecio (groundsel) measured by the pressure bomb technique. New Phytol. 95, 179–188.

Sapes, G., Sala, A., 2020. Relative water content consistently predicts drought mortality risk in seedling populations with different morphology, physiology, and times to death. bioRxv. https://doi.org/10.1101/2020.12.08.416917.
Sapes, G., Roskilly, B., Dobrowski, S., Maneta, M., Anderegg, W.R.L., Martinez-Vilalta, J., Sala, A., 2019. Plant water content integrates hydraulics and carbon depletion to predict drought-induced seedling mortality. Tree Physiol. 39, 1300–1312.
Savi, T., Marin, M., Luglio, J., Petruzzellis, F., Mayr, S., Nardini, A., 2016. Leaf hydraulic vulnerability protects stem functionality under drought stress in *Salvia officinalis*. Funct. Plant Biol. 43, 370–379.
Scoffoni, C., Pou, A., Aasamaa, K., Sack, L., 2008. The rapid light response of leaf hydraulic conductance: new evidence from two experimental methods. Plant Cell Environ. 31, 1803–1812.
Scoffoni, C., Rawls, M., McKown, A., Cochard, H., Sack, L., 2011. Decline of leaf hydraulic conductance with dehydration: relationship to leaf size and venation architecture. Plant Physiol. 156, 832–843.
Scoffoni, C., Vuong, C., Diep, S., Cochard, H., Sack, L., 2014. Leaf shrinkage with dehydration: coordination with hydraulic vulnerability and drought tolerance. Plant Physiol. 164, 1772–1788.
Scoffoni, C., Chatelet, D.S., Pasquet-Kok, J., et al., 2016. Hydraulic basis for the evolution of photosynthetic productivity. Nature Plants 2, 16072.
Scoffoni, C., Albuquerque, C., Brodersen, C.R., et al., 2017a. Outside-xylem vulnerability, not xylem embolism, controls leaf hydraulic decline during dehydration. Plant Physiol. 173, 1197–1210.
Scoffoni, C., Sack, L., Ort, D., 2017b. The causes and consequences of leaf hydraulic decline with dehydration. J. Exp. Bot. 68, 4479–4496.
Scoffoni, C., Albuquerque, C., Cochard, H., et al., 2018. The causes of leaf hydraulic vulnerability and its influence on gas exchange in Arabidopsis thaliana. Plant Physiol. 178, 1584–1601.
Skelton, R.P., Brodribb, T.J., Choat, B., 2017. Casting light on xylem vulnerability in an herbaceous species reveals a lack of segmentation. New Phytol. 214, 561–569.
Stocker, B.D., Zscheischler, J., Keenan, T.F., Prentice, I.C., Seneviratne, S.I., Peñuelas, J., 2019. Drought impacts on terrestrial primary production underestimated by satellite monitoring. Nat. Geosci. 12, 264–270.
Tombesi, S., Nardini, A., Farinelli, D., Palliotti, A., 2014. Relationships between stomatal behavior, xylem vulnerability to cavitation and leaf water relations in two cultivars of Vi*tis vinifera*. Physiol. Plantarum 152, 453–464.
Tramblay, Y., Koutroulisb, A., Samaniegoc, L., et al., 2020. Challenges for drought assessment in the Mediterranean region under future climate scenarios. Earth Sci. Rev. 210, 103348.
Trifilò, P., Nardini, A., Lo Gullo, M.A., Barbera, P.M., Raimondo, F., 2015. Diurnal changes in embolism rate in nine dry forest trees: relationship with specie-specific xylem vulnerability, hydraulic strategy and wood traits. Tree Physiol. 35, 694–705.
Trifilò, P., Raimondo, F., Savi, T., Lo Gullo, M.A., Nardini, A., 2016. The contribution of vascular and extra-vascular water pathways to drought-induced decline of leaf hydraulic conductance. J. Exp. Bot. 67, 5029–5039.
Trifilò, P., Petruzzellis, F., Abate, E., Nardini, A., 2020. The Extra-vascular Water Pathway Regulates Dynamic Leaf Hydraulic Decline and Recovery in *Populus nigra*. https://doi.org/10.1111/ppl.13266.
Trueba, S., Pan, R., Scoffoni, C., John, G.P., Davis, S.D., Sack, L., 2019. Thresholds for leaf damage due to dehydration: declines of hydraulic function, stomatal conductance and cellular integrity precede those for photochemistry. New Phytol. 223, 134–149.
Tyree, M.T., Hammel, H.T., 1972. The measurement of the turgor pressure and the water relations of plants by the pressure-bomb technique. J. Exp. Bot. 3, 267–282.
Underwood, E.C., Viers, J.H., Klausmeyer, K.R., Cox, R.L., Shaw, M.R., 2009. Threats and biodiversity in the mediterranean biome. Divers. Distrib. 15, 188–197.
Urli, M., Porte, A.J., Cochard, H., Guengant, Y., Burlett, R., Delzon, S., 2013. Xylem embolism threshold for catastrophic hydraulic failure in angiosperm trees. Tree Physiol. 33, 672–683.
Wang, X., Du, T., Huang, J., Peng, S., Xiong, D., 2018. Leaf hydraulic vulnerability triggers the decline in stomatal and mesophyll conductance during drought in rice. J. Exp. Bot. 69, 4033–4045.
Xiong, D., Nadal, M., 2020. Linking water relations and hydraulics with photosynthesis. Plant J. 101, 800–815.
Xiong, D., Douthe, C., Flexas, J., 2018. Differential coordination of stomatal conductance, mesophyll conductance, and leaf hydraulic conductance in response to changing light across species. Plant Cell Environ. 41, 436–450.